Electronic Supplementary Information

Historical Account of Dinitrogen-bridged Diiron Complex Synthesis using a Commercial Tripodal Ligand

Nathan C. Smythe,*[a] Joydeb Mondal,[b] Juan G. Duque,[a] Russell K. Feller,[c] Marco Flores,[b] John C. Gordon,*[d] Neil J. Henson,[e] Moshe Paz-Pasternak,[f] Francisca N. Rein,[a] Brian L. Scott,[c] R. Dean Taylor,[c] Ryan J. Trovitch*[b]

a. Chemistry Division, Los Alamos National Laboratory, Los Alamos, NM 87545, USA.
b. School of Molecular Sciences, Arizona State University, Tempe, AZ 85287, USA.
c. Materials Physics and Applications Division, Los Alamos National Laboratory, Los Alamos, NM 87545, USA.
d. Chemistry Division, Brookhaven National Laboratory, Upton, NY 11973, USA.
e. Theoretical Division, Los Alamos National Laboratory, Los Alamos, NM 87545, USA.
f. School of Physics and Astronomy, Tel Aviv University, 69978 Tel Aviv, Israel.

**e-mail: nsmythe@lanl.gov, jgordon1@bnl.gov, ryan.trovitch@asu.edu*

EXPERIMENTAL DETAILS

General Considerations: Unless otherwise stated, synthetic manipulations were performed in an MBraun Glovebox under an atmosphere of purified argon (LANL) or nitrogen (ASU). Toluene was purchased from Oakwood Chemicals, purified using a Pure Process Technology solvent system, and dried in the glovebox over 4Å molecular sieves and potassium before use. Benzene-d_6 was obtained from Oakwood Chemicals, degassed through three freeze-pump-thaw cycles, and stored over activated 4Å molecular sieves and potassium in the glovebox before use. Anhydrous $FeCl_2$ (Sigma-Aldrich), 1,1,1-tris(diphenylphosphinomethyl)ethane (Triphos, Strem Chemicals), and potassium (Oakwood Chemicals) were used as received. Graphite and boron nitride (BN) were purchased from commercial sources and dried *in vacuo* while heating. $^{15}N_2$ and H_2 were used as received. (Triphos)$FeCl_2$ (**1**)[1] and (Triphos)Fe(μ-H)$_3$Fe(μ-H)$_3$Fe(Triphos) (**3**)[2] have been structurally characterized elsewhere, but alternate syntheses are presented here.

Solution nuclear magnetic resonance (NMR) spectra were recorded at room temperature on a Varian 400, Bruker 500, or Bruker 600 MHz NMR spectrometer. All ^{1}H NMR and ^{13}C NMR chemical shifts (ppm) are reported relative to $SiMe_4$ using ^{1}H (residual) and ^{13}C chemical shifts of the solvent as secondary standards. ^{31}P NMR shifts are reported relative to H_3PO_4 using the absolute ^{1}H NMR frequency of an internal $Si(CH_3)_4$ standard. Elemental analyses were performed by Atlantic Microlab, Inc. (Norcross, GA). Resonance Raman spectra were collected using a 1:1 sample to BN mixture using a 514 nm excitation wavelength. Mössbauer spectrometry (^{57}Fe) was performed in constant acceleration mode using a liquid helium cryostat and conventional data analysis programs. A ^{57}Co in Rh source provided the 14.4 KeV recoil-free Mössbauer effect γ-rays. The samples were contained in an O-ring sealed Lucite holder under an Ar atmosphere. The source and absorber were held at the same temperature for data taken over the range 1.5 to 300 K.

X-ray Crystallography. Single crystals suitable for X-ray diffraction were coated with polyisobutylene oil in the glovebox and transferred to glass fiber with Apiezon N grease, which was then mounted on the goniometer head of a Bruker D8 Venture κ-geometry diffractometer (ASU) equipped with Mo Kα radiation and a multilayer mirror monochromator. A full sphere strategy was used to collect data and determine the lattice constants. The space group was identified and the data was processed using the Bruker SAINT software package and corrected for absorption effects using SADABS. The structures were solved using intrinsic phasing methods (SHELXT) completed by subsequent Fourier synthesis and refined by full-matrix, least-squares procedures on [F2] (SHELXL).

SYNTHETIC PROCEDURES

Alternate Preparation of (Triphos)$FeCl_2$ (1): Anhydrous $FeCl_2$ (0.203 g, 1.60 mmol) and 1,1,1-tris(diphenylphosphinomethyl)ethane (1.00 g, 1.60 mmol) were added to a Schlenk tube followed by ca. 100 mL of toluene in a glovebox. The tube was sealed and then heated to 100 °C for ca. 72 h until the $FeCl_2$ had been solubilized to afford a very light green solution. The reaction mixture was then filtered through Celite and **1** was isolated as a colorless crystalline solid by concentrating the solution and storing it in the glovebox freezer at -35 °C (80%, 0.962 g, 1.28 mmol). Anal. Calc'd. C: 65.53%, H: 5.23%, Cl: 9.44%; Found C: 65.81%, H: 5.23%, Cl: 9.25%. ^{1}H NMR (400 MHz, benzene-d_6): 12.44 (peak width at half-height = 673 Hz), 7.46 (35 Hz), 2.67 (47 Hz).

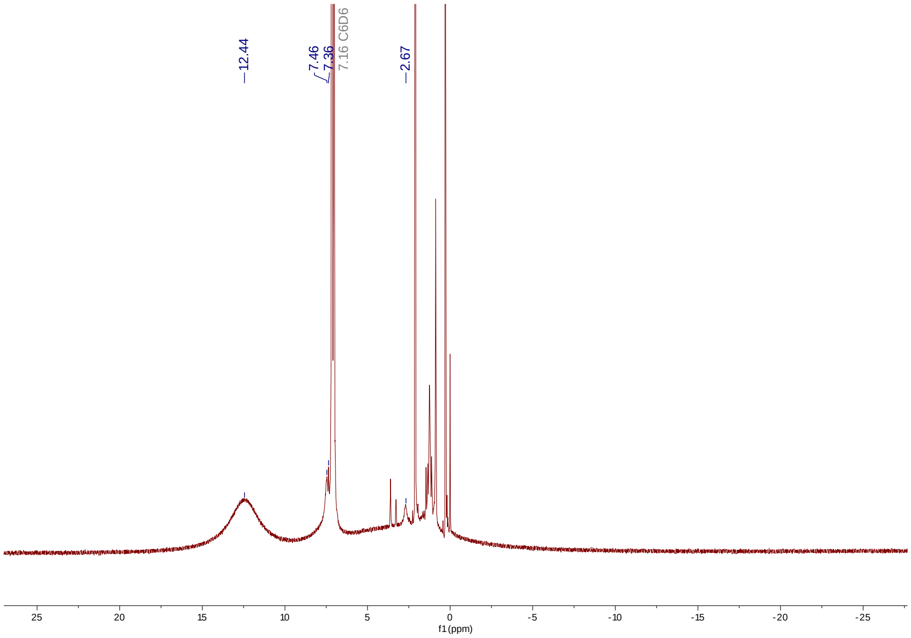

Figure S1. ^{1}H NMR spectrum of **1** in benzene-d_6 at 23 °C.

Preparation of [(Triphos)Fe]$_2$(μ-N_2) (2): *Method 1:* Compound **1** (0.500 g, 0.67 mmol) and KC_8 (184 mg, 1.36 mmol) along with a glass-coated stir bar were added to a Fischer-Porter tube which was subsequently attached to a transfer bridge and evacuated. Toluene (ca. 50 mL) was vacuum transferred onto the solids and kept frozen. A N_2 cylinder was attached to the transfer bridge, the tube was pressurized to 3.4 atm (50 psi) of N_2, and the toluene allowed to thaw with stirring. The mixture became dark red. Once the reaction returned to room temperature, it was immediately moved into a glovebox and filtered through Celite. The Celite was washed with toluene until the solvent was nearly colorless. The solution was then concentrated and crystallized in the glovebox freezer at -35 °C and washed with cold toluene followed by cold Et_2O (40%, 0.370 g, 0.266 mmol). This procedure was repeated under $^{15}N_2$ to obtain **[(Triphos)Fe]$_2$(*μ*-^{15}N$_2$) (2-^{15}N$_2$)**. *Method 2:* Into a 20 mL vial, 0.276 g (0.367 mmol) of **1** was weighed and dissolved in 10 mL of toluene. This solution was then transferred to a Parr reactor, an additional 20 mL toluene was added, and cooled to -196 ℃ in a liquid nitrogen-cooled cold well for 1 h. After this time, 0.102 g KC_8 (0.752 mmol) was weighed out and transferred to the reactor so that it sat on top of the frozen solution of **1**. The reactor was quickly sealed, removed from the glovebox, and cooled with liquid nitrogen again. Then, the reactor was pressurized with 50 psi of N_2 gas and then allowed to stir upon warming to ambient temperature. The reactor was quickly taken into the glovebox, and the resulting blood-red solution was filtered through Celite and concentrated under reduced pressure. Allowing the solution to stand at -35 ℃ overnight resulted in lustrous green block-shaped crystals suitable for single-crystal X-ray diffraction. Yield: 0.101 g (20%). Satisfactory elemental analysis could not be obtained due to decomposition (N_2 loss). Resonance Raman: ν_{NN} = 1503 cm^{-1}, $\nu_{15N\text{-}15N}$ = 1450 cm^{-1}. ^{1}H NMR (500 MHz, benzene-d_6): 7.71 (s, 14H, *phenyl*), 7.58-7.49 (m, 7H, *phenyl*), 7.05-7.01 (m, 19H, *phenyl*), 6.92-6.89 (t, J = 7.5 Hz, 14H, *phenyl*), 6.82-6.79 (t, J = 7.3 Hz, 8H, *phenyl*), 2.11 (s, 12H, CH_2), 1.36 (s, 6H, CH_3). ^{13}C NMR (150.90 MHz, benzene-d_6): 140.66 (s, *phenyl*), 133.57 (d, J = 20.5 Hz, *phenyl*), 129.34 (s, *phenyl*), 30.23 (s, $C(CH_2)_3CH_3$), 25.89 (dt, J_{CP} = 19.0 Hz, CH_2), 14.28 (s, CH_3). ^{31}P NMR (202.46 MHz, benzene-d_6): 71.34 (s, Fe-P). ^{57}Fe Mössbauer (62 K): δ = -0.09 mm/s, ΔE_Q = 0.41 mm/s.

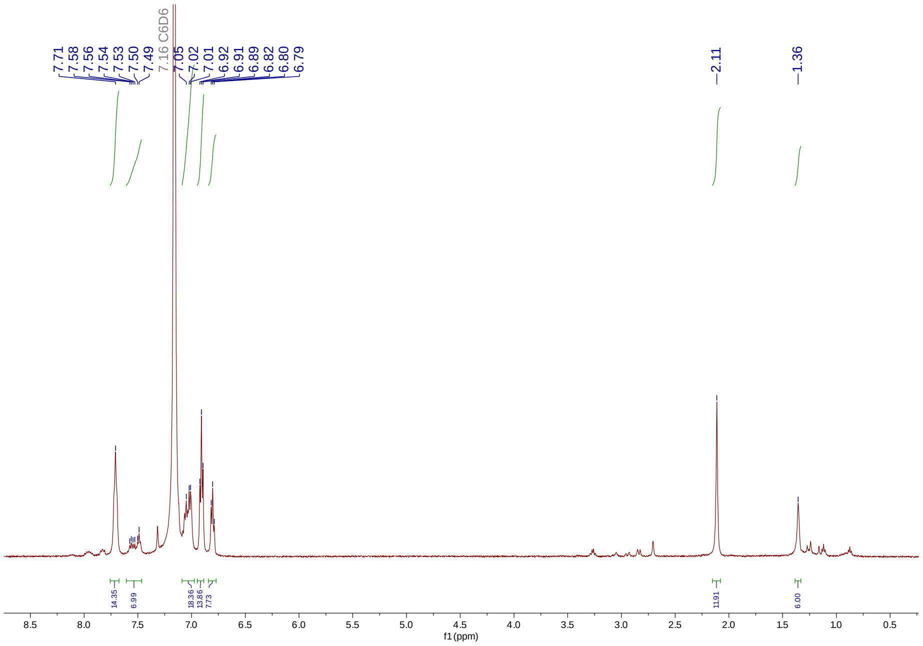

Figure S2. ^{1}H NMR spectrum of **2** in benzene-d_6.

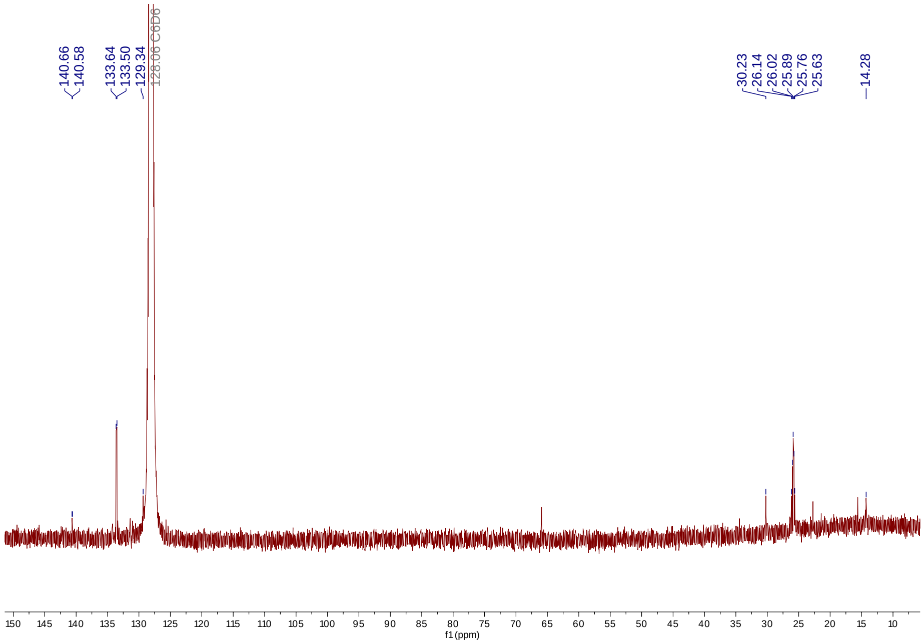

Figure S3. ^{13}C NMR spectrum of **2** in benzene-d_6.

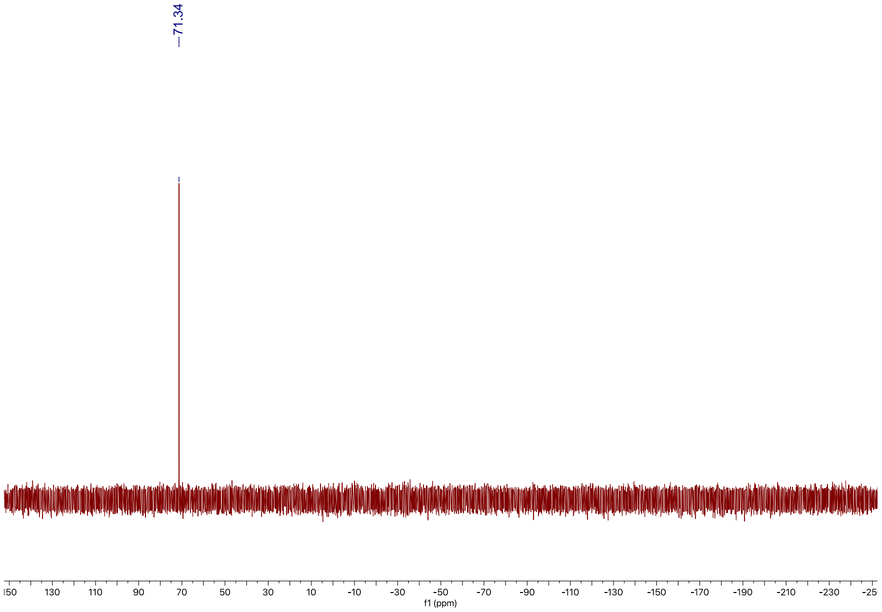

Figure S4. ^{31}P NMR spectrum of **2** in benzene-d_6.

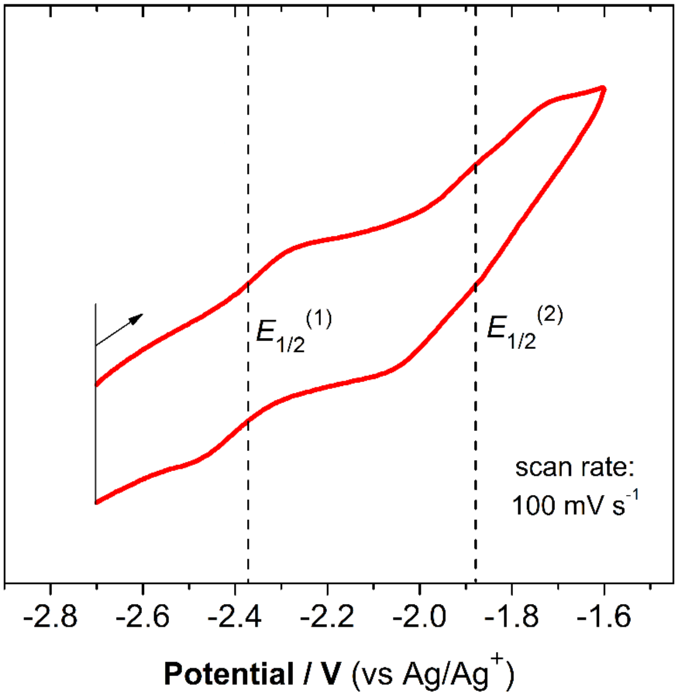

Figure S5. Cyclic voltammogram of **2** in fluorobenzene, 0.1 M NBu_4PF_6. The mid-potentials for Fe(0)-Fe(0) → Fe(0)-Fe(I) ($E_{1/2}^{(1)}$) and Fe(0)-Fe(I) → Fe(I)-Fe(I) ($E_{1/2}^{(2)}$) are -2.37 V and -1.88 V, respectively.

Alternate Preparation of (Triphos)Fe(μ-H)$_3$Fe(μ-H)$_3$Fe(Triphos) (3): Compound **2** (0.200 g, 0.14 mmol) was added to a Schlenk flask and dissolved in ca. 50 mL of toluene. The solution was degassed and H_2 (ca. 1 atm) was added. The solution was allowed to stir at room temperature for 2 days. Afterwards, the solution was filtered through Celite, concentrated, and crystallized in the glovebox freezer. The product was washed with cold toluene (0.063 g, 0.044 mmol, 61%). Anal. calc'd C: 69.22%, H: 5.95%; Found C: 69.16%, H: 5.71%. ^{1}H NMR (500 MHz, benzene-d_6, 25 °C): Paramagnetic compound = 76.00 (peak width at half maxima = 828 Hz), 48.42 (286 Hz), -8.58 (117 Hz), -16.80 (187 Hz); Diamagnetic compound = 7.29 (br m, 24H, *phenyl*), 7.07-7.01 (m, 16H, *phenyl*), 6.97 (m, 20H, *phenyl*), 1.98 (s, 12H, -CH_2), 0.95 (s, 6H, -CH_3), -16.54 (s, 2H, Fe-*H*). ^{13}C NMR (125.76 MHz, benzene-d_6, 25 °C, diamagnetic compound): 146.02 (s, *phenyl*), 134.20 (s, *phenyl*), 126.74 (s, *phenyl*), 42.93 (s, -$C(CH_2)_3CH_3$), 36.55 (s, -CH_2), 25.89 (s, -CH_3). ^{31}P NMR (202.46 MHz, benzene-d_6, 25 °C, diamagnetic compound): 58.38 (s, Fe-*P*). Mossbauer (75 K): Component 1 (72%), δ = -0.01 mm/s, ΔE_Q = 0.51 mm/s; Component 2 (28%), δ = -0.10 mm/s, ΔE_Q = 0.18 mm/s.

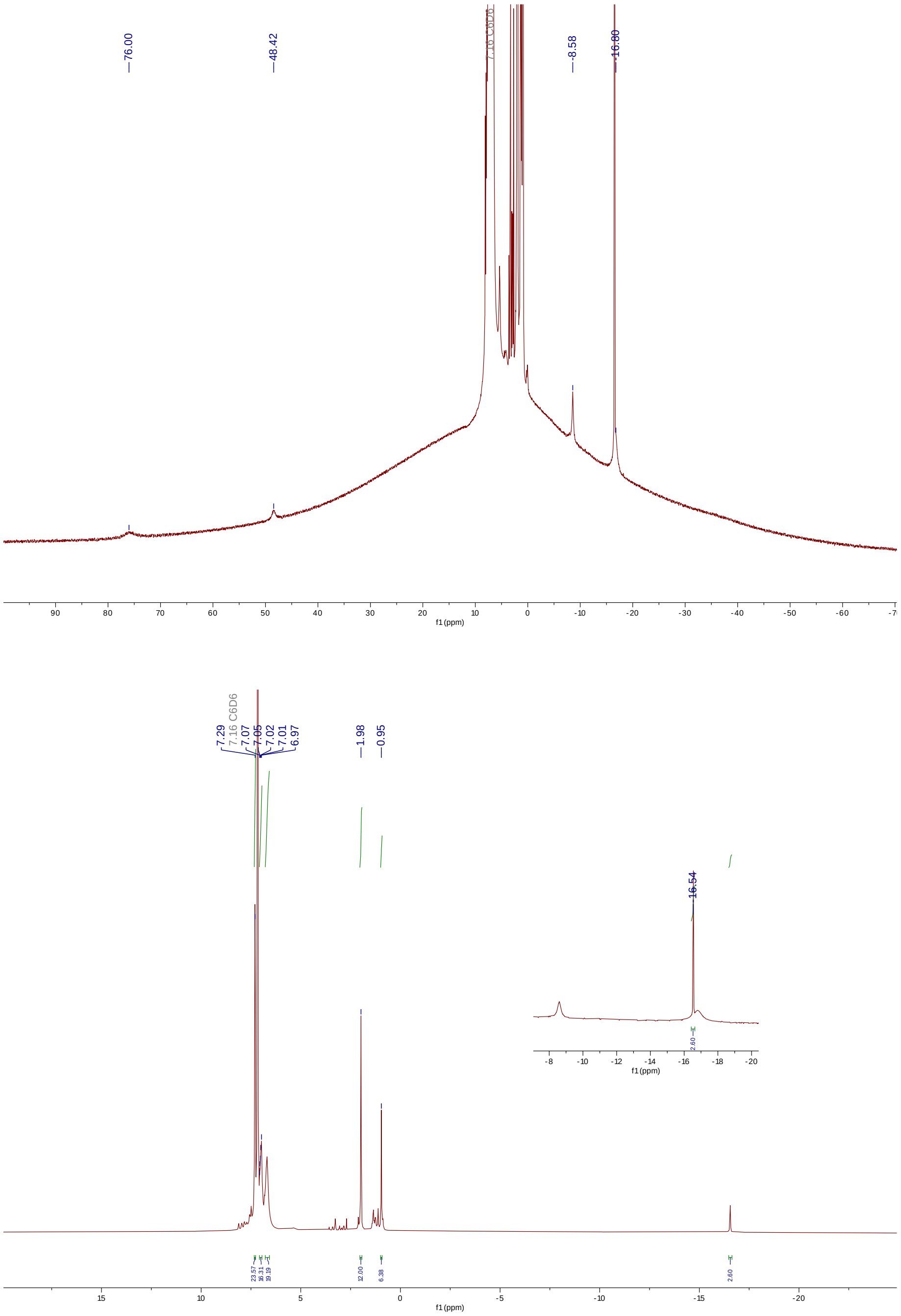

Figure S6. Two representations of the same ^{1}H NMR spectrum of **3** in benzene-d_6 at 25 °C. The top representation highlights the paramagnetically shifted and broadened peaks attributed to **3**, while the bottom representation offers integrations for the diamagnetic compound proposed to be (Triphos)Fe(μ-H)$_2$Fe(Triphos).

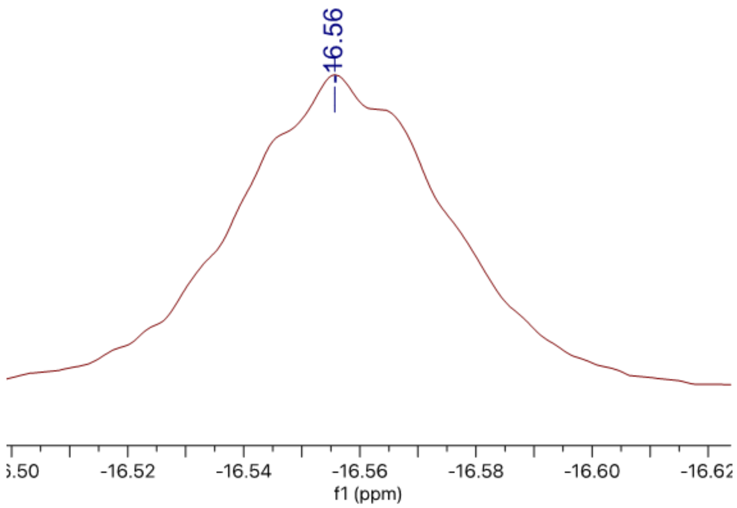

Figure S7. Weakly-resolved ^{1}H NMR septet for the hydride peak of (Triphos)Fe(μ-H)$_2$Fe(Triphos) with ^{31}P coupling in benzene-d_6.

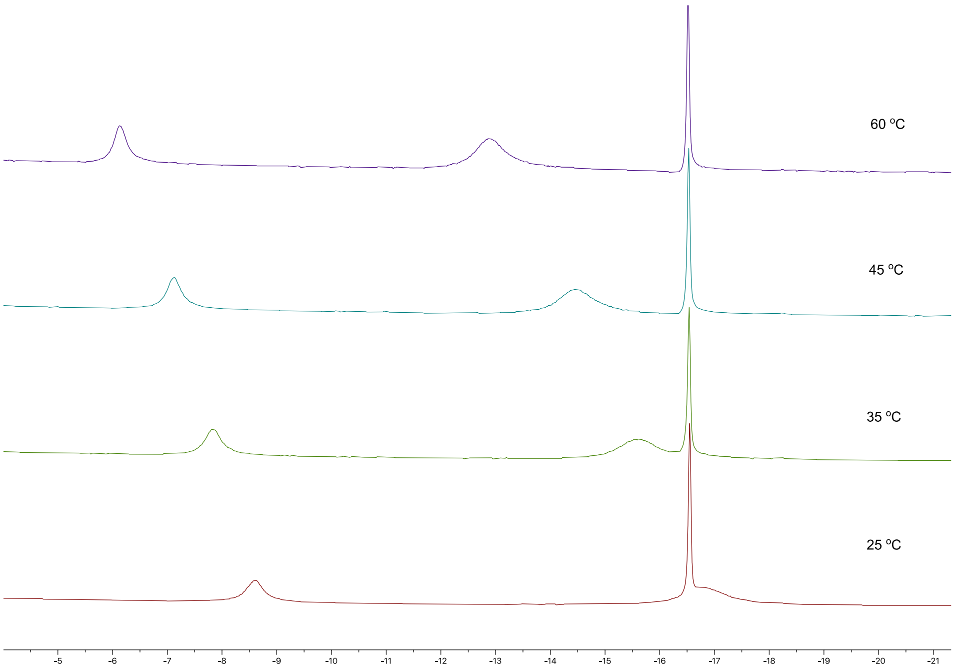

Figure S8. Variable temperature ^{1}H NMR spectrum of **3** (broad peaks) and (Triphos)Fe(μ-H)$_2$Fe(Triphos) (sharp peak) in benzene-d_6.

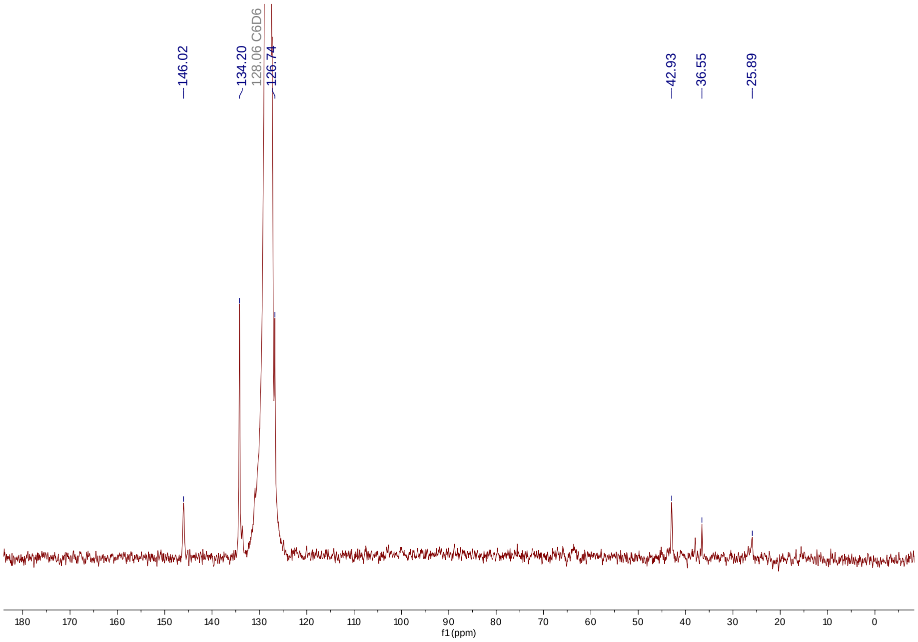

Figure S9. ^{13}C NMR spectrum of (Triphos)Fe(μ-H)$_2$Fe(Triphos) in benzene-d_6, as observed for solution of **3**.

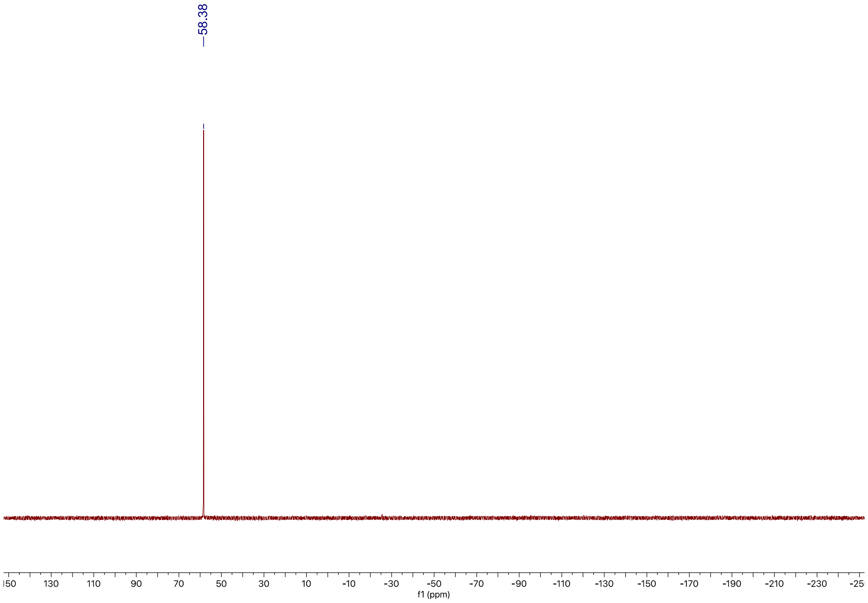

Figure S10. ^{31}P NMR spectrum of (Triphos)Fe(μ-H)$_2$Fe(Triphos) in benzene-d_6, as observed for solution of **3**.

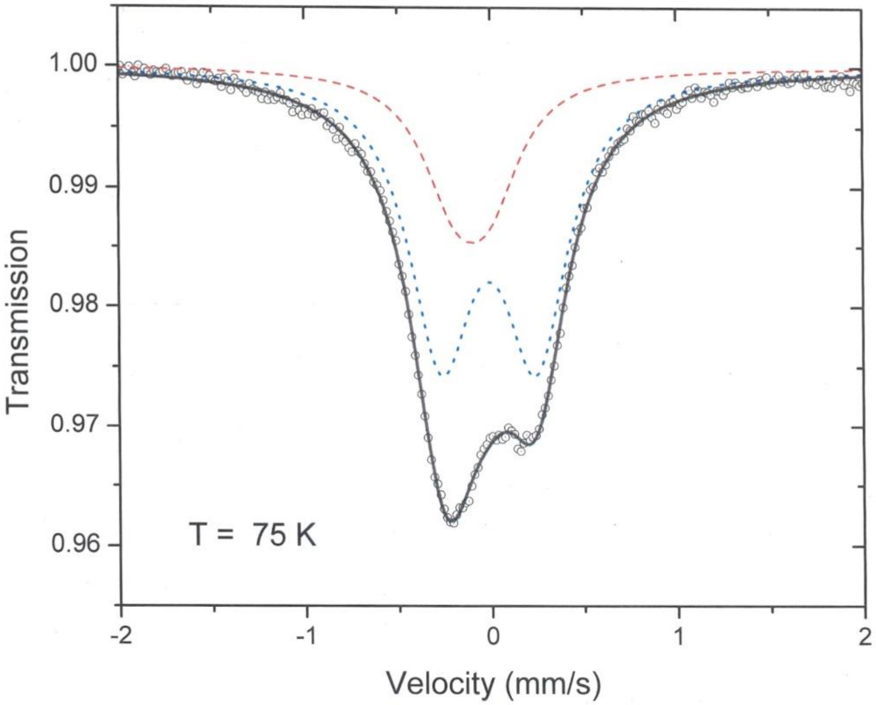

Figure S11. Mössbauer spectrum of **3** at 75 K.

CRYSTALLOGRAPHIC TABLES

Table S1. Crystallographic Data for **2**.

	2
chemical formula	$C_{82}H_{78}Fe_2P_6$
formula weight	1388.98
crystal dimensions	0.141 × 0.119 × 0.080
crystal system	monoclinic
space group	P 1 21/c 1
a (Å)	22.7264(5)
b (Å)	15.2574(3)
c (Å)	21.1376(4)
α (deg)	90
β (deg)	108.9700(10)
γ (deg)	90
V (Å^3)	6931.3(2)
Z	4
T (K)	100.(2)
ρ_{calcd} (g cm^{-3})	1.331
μ (mm^{-1})	0.604
reflections collected	349913
data/restraints/parameters	12710/0/831
R_1 [$I > 2\sigma(I)$]	0.0329
wR_2 (all data)	0.0894
Goodness-of-fit	1.033
Largest peak, hole (eÅ^{-3})	0.893, -0.493

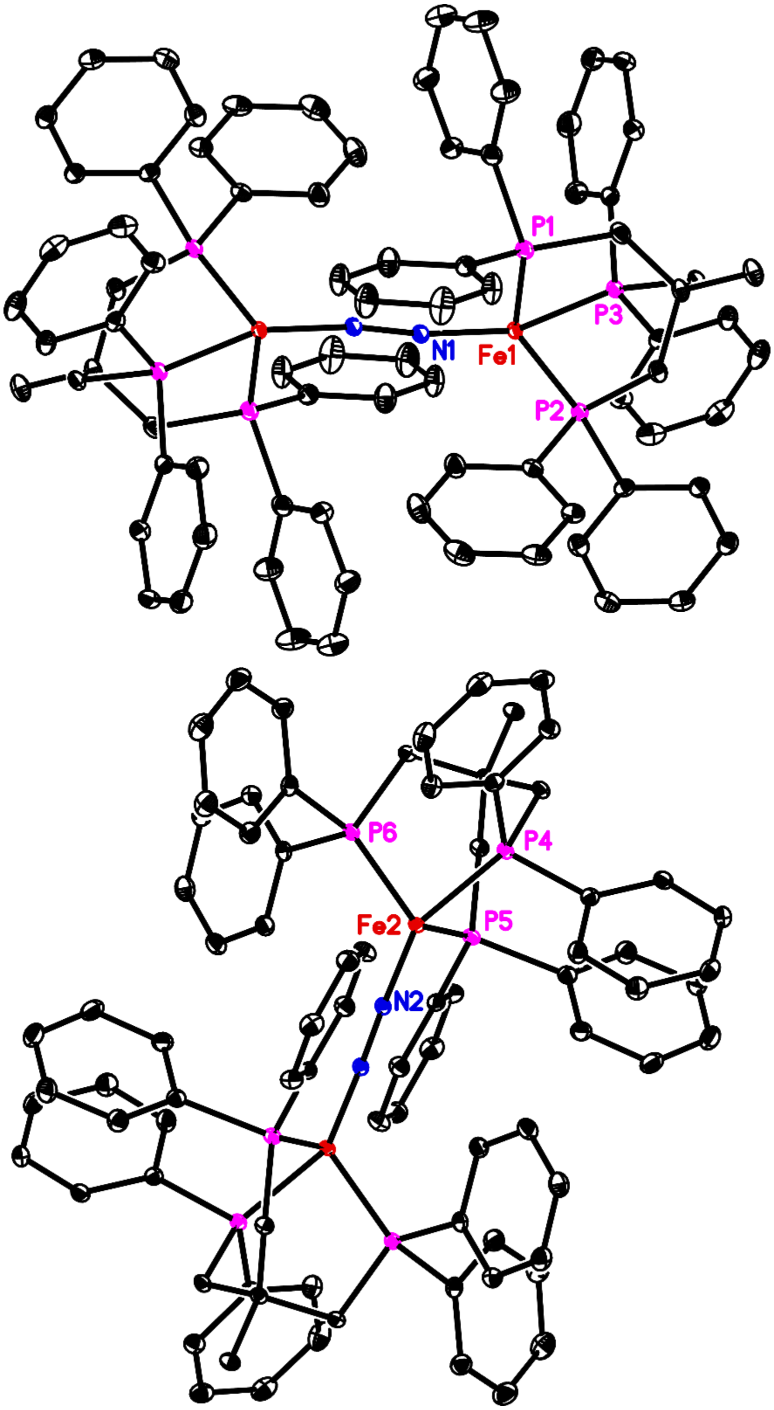

Figure S12. The molecular structure of **2** displayed at 30% probability ellipsoids. Atoms generated by symmetry are included, but not labeled. Hydrogen atoms are omitted for clarity.

Table S2. Bond lengths (Å) and angles (°) determined for **2**.

Fe1-N1	1.7361(16)	C8-C9	1.385(3)	C45-C46	1.375(3)
Fe1-P1	2.1186(6)	C9-C10	1.373(3)	C46-C47	1.386(3)
Fe1-P2	2.1415(5)	C10-C11	1.370(4)	C48-C53	1.388(3)
Fe1-P3	2.1546(6)	C11-C12	1.396(3)	C48-C49	1.397(3)
Fe2-N2	1.7251(15)	C13-C14	1.390(3)	C49-C50	1.386(3)
Fe2-P5	2.1407(5)	C13-C18	1.396(3)	C50-C51	1.384(3)
Fe2-P6	2.1449(5)	C14-C15	1.393(3)	C51-C52	1.380(3)
Fe2-P4	2.1521(5)	C15-C16	1.382(4)	C52-C53	1.392(3)
P1-C7	1.842(2)	C16-C17	1.383(4)	C54-C59	1.388(3)
P1-C37	1.852(2)	C17-C18	1.390(3)	C54-C55	1.399(3)
P1-C1	1.862(2)	C19-C20	1.392(3)	C55-C56	1.386(3)
P2-C19	1.845(2)	C19-C24	1.396(3)	C56-C57	1.389(3)
P2-C13	1.846(2)	C20-C21	1.390(3)	C57-C58	1.379(3)
P2-C38	1.862(2)	C21-C22	1.380(3)	C58-C59	1.385(3)
P3-C31	1.847(2)	C22-C23	1.380(3)	C60-C61	1.389(3)
P3-C25	1.848(2)	C23-C24	1.394(3)	C60-C65	1.398(3)
P3-C39	1.8632(19)	C25-C26	1.391(3)	C61-C62	1.389(3)
P4-C48	1.8453(19)	C25-C30	1.394(3)	C62-C63	1.385(3)
P4-C42	1.8526(19)	C26-C27	1.390(3)	C63-C64	1.381(3)
P4-C78	1.8611(18)	C27-C28	1.380(4)	C64-C65	1.385(3)
P5-C60	1.8405(19)	C28-C29	1.382(3)	C66-C67	1.395(3)
P5-C54	1.847(2)	C29-C30	1.391(3)	C66-C71	1.397(3)
P5-C79	1.8537(19)	C31-C36	1.391(3)	C67-C68	1.386(3)
P6-C72	1.842(2)	C31-C32	1.402(3)	C68-C69	1.385(3)
P6-C80	1.8475(18)	C32-C33	1.388(3)	C69-C70	1.387(3)
P6-C66	1.8501(19)	C33-C34	1.384(4)	C70-C71	1.392(3)
N1-N1A	1.208(3)	C34-C35	1.373(4)	C72-C77	1.394(3)
N2-N2A	1.207(3)	C35-C36	1.395(3)	C72-C73	1.396(3)
C1-C2	1.385(3)	C37-C40	1.557(3)	C73-C74	1.385(3)
C1-C6	1.388(3)	C38-C40	1.544(3)	C74-C75	1.382(3)
C2-C3	1.388(3)	C39-C40	1.542(3)	C75-C76	1.381(3)
C3-C4	1.375(3)	C40-C41	1.539(3)	C76-C77	1.393(3)
C4-C5	1.382(4)	C42-C43	1.389(3)	C78-C81	1.549(2)
C5-C6	1.401(3)	C42-C47	1.398(3)	C79-C81	1.551(3)
C7-C12	1.373(3)	C43-C44	1.398(3)	C80-C81	1.551(3)
C7-C8	1.393(3)	C44-C45	1.388(3)	C81-C82	1.537(2)

N1-Fe1-P1	106.16(6)	C7-P1-C1	100.18(9)	C25-P3-C39	100.46(9)
N1-Fe1-P2	128.33(5)	C37-P1-C1	103.87(10)	C31-P3-Fe1	117.27(7)
P1-Fe1-P2	93.33(2)	C7-P1-Fe1	115.49(7)	C25-P3-Fe1	121.23(7)
N1-Fe1-P3	135.65(5)	C37-P1-Fe1	115.97(7)	C39-P3-Fe1	114.56(6)
P1-Fe1-P3	90.80(2)	C1-P1-Fe1	113.55(7)	C48-P4-C42	96.41(8)
P2-Fe1-P3	89.90(2)	C19-P2-C13	99.55(9)	C48-P4-C78	104.28(9)
N2-Fe2-P5	116.11(5)	C19-P2-C38	103.85(9)	C42-P4-C78	101.25(9)
N2-Fe2-P6	126.57(5)	C13-P2-C38	100.20(9)	C48-P4-Fe2	115.63(6)
P5-Fe2-P6	92.30(2)	C19-P2-Fe1	118.40(6)	C42-P4-Fe2	122.34(7)
N2-Fe2-P4	131.13(5)	C13-P2-Fe1	118.13(7)	C78-P4-Fe2	114.02(6)
P5-Fe2-P4	88.38(2)	C38-P2-Fe1	113.98(7)	C60-P5-C54	96.27(9)
P6-Fe2-P4	90.95(2)	C31-P3-C25	96.76(9)	C60-P5-C79	103.05(9)
C7-P1-C37	105.99(10)	C31-P3-C39	103.36(9)	C54-P5-C79	105.31(9)

C60-P5-Fe2	121.12(7)
C54-P5-Fe2	115.42(6)
C79-P5-Fe2	113.28(6)
C72-P6-C80	103.00(9)
C72-P6-C66	100.20(9)
C80-P6-C66	103.19(9)
C72-P6-Fe2	117.42(6)
C80-P6-Fe2	114.16(6)
C66-P6-Fe2	116.70(6)
N1A-N1-Fe1	166.0(2)
N2A-N2-Fe2	172.32(19)
C2-C1-C6	119.4(2)
C2-C1-P1	118.13(16)
C6-C1-P1	122.52(18)
C1-C2-C3	120.9(2)
C4-C3-C2	119.3(2)
C3-C4-C5	120.9(2)
C4-C5-C6	119.6(2)
C1-C6-C5	119.9(2)
C12-C7-C8	118.4(2)
C12-C7-P1	124.84(17)
C8-C7-P1	116.40(16)
C9-C8-C7	120.7(2)
C10-C9-C8	120.4(2)
C11-C10-C9	119.4(2)
C10-C11-C12	120.5(2)
C7-C12-C11	120.6(2)
C14-C13-C18	118.69(19)
C14-C13-P2	119.69(15)
C18-C13-P2	121.62(16)
C13-C14-C15	120.4(2)
C16-C15-C14	120.5(2)
C15-C16-C17	119.6(2)
C16-C17-C18	120.1(2)
C17-C18-C13	120.7(2)
C20-C19-C24	118.15(18)
C20-C19-P2	117.47(15)
C24-C19-P2	124.05(15)
C21-C20-C19	120.7(2)
C22-C21-C20	120.5(2)
C23-C22-C21	119.8(2)
C22-C23-C24	119.9(2)
C23-C24-C19	120.95(19)
C26-C25-C30	118.63(19)
C26-C25-P3	119.60(16)
C30-C25-P3	121.75(16)
C27-C26-C25	120.3(2)
C28-C27-C26	120.5(2)
C27-C28-C29	120.0(2)
C28-C29-C30	119.7(2)
C29-C30-C25	120.9(2)
C36-C31-C32	117.99(19)
C36-C31-P3	124.48(17)
C32-C31-P3	117.46(16)
C33-C32-C31	120.8(2)
C34-C33-C32	120.3(2)
C35-C34-C33	119.7(2)
C34-C35-C36	120.4(2)
C31-C36-C35	120.8(2)
C40-C37-P1	115.22(14)
C40-C38-P2	116.18(13)
C40-C39-P3	115.94(13)
C41-C40-C39	107.17(16)
C41-C40-C38	107.72(16)
C39-C40-C38	112.31(16)
C41-C40-C37	107.20(16)
C39-C40-C37	110.60(16)
C38-C40-C37	111.56(16)
C43-C42-C47	118.92(18)
C43-C42-P4	119.57(15)
C47-C42-P4	121.44(15)
C42-C43-C44	120.0(2)
C45-C44-C43	119.9(2)
C46-C45-C44	120.5(2)
C45-C46-C47	119.6(2)
C46-C47-C42	121.0(2)
C53-C48-C49	118.35(18)
C53-C48-P4	125.90(15)
C49-C48-P4	115.74(15)
C50-C49-C48	120.74(19)
C51-C50-C49	120.35(19)
C52-C51-C50	119.41(19)
C51-C52-C53	120.42(19)
C48-C53-C52	120.70(18)
C59-C54-C55	118.11(19)
C59-C54-P5	124.94(16)
C55-C54-P5	116.95(15)
C56-C55-C54	120.8(2)
C55-C56-C57	120.2(2)
C58-C57-C56	119.4(2)
C57-C58-C59	120.4(2)
C58-C59-C54	121.1(2)
C61-C60-C65	119.08(18)
C61-C60-P5	118.63(15)
C65-C60-P5	121.94(15)
C62-C61-C60	120.33(19)
C63-C62-C61	120.0(2)
C64-C63-C62	120.20(19)
C63-C64-C65	120.00(19)
C64-C65-C60	120.37(19)
C67-C66-C71	118.46(18)
C67-C66-P6	117.88(14)
C71-C66-P6	123.66(15)
C68-C67-C66	120.82(19)
C69-C68-C67	120.4(2)
C68-C69-C70	119.51(19)
C69-C70-C71	120.26(19)
C70-C71-C66	120.53(19)
C77-C72-C73	118.22(18)
C77-C72-P6	125.54(15)
C73-C72-P6	116.14(15)
C74-C73-C72	120.9(2)
C75-C74-C73	120.1(2)
C76-C75-C74	120.0(2)
C75-C76-C77	119.9(2)
C76-C77-C72	120.8(2)
C81-C78-P4	114.19(13)
C81-C79-P5	113.89(12)
C81-C80-P6	113.95(13)
C82-C81-C78	107.47(15)
C82-C81-C80	106.61(15)
C78-C81-C80	110.62(15)
C82-C81-C79	108.65(15)
C78-C81-C79	111.25(15)
C80-C81-C79	112.01(15)

REFERENCES

1. A. Petuker, K. Merz, C. Merten and U.-P. Apfel, *Inorg. Chem.* 2016, **55**, 1183-1191.

2. L. Iffland, A. Khedkar, A. Petuker, M. Lieb, F. Wittkamp, M. van Gastel, M. Roemelt and U.-P. Apfel, *Organometallics*, 2019, **38**, 289-299.